PROCEEDINGS OF SCIENCE

# Precise predictions for $\Lambda_b \to \Lambda_c \ell^- \bar{\nu}_\ell$ decays

**William Sutcliffe**[*][†]
*Karlsruhe Institute of Technology*
*E-mail:* william.sutcliffe2@kit.edu

These proceedings summarise recent work in which the Standard Model and New Physics form factors of $\Lambda_b \to \Lambda_c \ell^- \bar{\nu}_\ell$ decays were computed up to order $\mathcal{O}(\Lambda^2_{\rm QCD}/m_c^2)$ using Heavy Quark Effective Theory (HQET). This allowed for a subsequent HQET-based determination of form factors of the decay using a fit, which combines recent theoretical predictions and experimental measurements. Consequently, the most precise value of $R(\Lambda_c)$ to date was determined, $R(\Lambda_c) = 0.324 \pm 0.004$. Additionally, the sensitivity of $R(\Lambda_c)$ to potential NP interactions was explored.

*European Physical Society Conference on High Energy Physics - EPS-HEP2019 -*
*10-17 July, 2019*
*Ghent, Belgium*

[*]Speaker.
[†]On behalf of my co-authors Florian Bernlochner, Zoltan Ligeti and Dean Robinson



https://pos.sissa.it/

PoS(EPS-HEP2019)265

## 1. Introduction

Recently, a number of anomalies in the decays of $B$ mesons have been observed, which can be explained potentially by the same underlying new physics (NP) [1, 2]. A particular example of this has been measurements of the ratio of branching fractions $R\left(D^{(*)}\right) = \mathcal{B}(B \to D^{(*)}\tau^-\bar{\nu}_\tau)/\mathcal{B}(B \to D^{(*)}\ell^-\bar{\nu}_\ell)$, for which the global average of measurements is $\sim 3\sigma$ above the Standard Model (SM) expectation [3]. At the LHC there is the unique possibility to study $B$ physics with the decays of $b$ baryons. In particular, around 20% of the $b$ hadrons measured by LHCb are actually $\Lambda_b^0$ baryons. Any new physics hints in $B$ meson decays should show up in their baryonic counterparts. This motivates the measurement of the baryonic ratios $R(\Lambda_c^{(*)}) = \mathcal{B}(\Lambda_b \to \Lambda_c^{(*)+}\tau^-\bar{\nu}_\tau)/\mathcal{B}(\Lambda_b \to \Lambda_c^{(*)+}\ell^-\bar{\nu}_\ell)$. A sensitivity study performed by LHCb concluded that a measurement of $R(\Lambda_c)$, would have the smallest relative uncertainty after the ratios $R(D)$ and $R(D^*)$ [4].

The SM and NP form factors form factors of $\Lambda_b \to \Lambda_c\ell^-\bar{\nu}_\ell$ were computed using LQCD in References [5, 6], respectively. These LQCD predictions yielded a prediction of $R(\Lambda_c) = 0.33 \pm 0.01$. On the experimental front, LHCb measured the differential spectrum of the decay [7] in momentum transfer squared, $q^2$. These proceedings summarise results from recent papers [8, 9], which utilised the aforementioned results within the framework of Heavy Quark Effective Theory (HQET) to determine the form factors of the decay $\Lambda_b \to \Lambda_c\mu^-\bar{\nu}_\mu$. This resulted in the most precise determination of $R(\Lambda_c)$ to date, $R(\Lambda_c) = 0.324 \pm 0.004$.

## 2. $\Lambda_b \to \Lambda_c\ell\nu$ in the SM and beyond

In the SM, the decay $\Lambda_b \to \Lambda_c\ell^-\bar{\nu}_\ell$ proceeds via the weak interaction with a $V$-$A$ structure. The influence of QCD on the hadronic matrix element for the $\Lambda_b \to \Lambda_c$ transition can be parametrised by 3 vector and 3 axial-vector form factors according to:

$$\begin{aligned}
\langle\Lambda_c(p',s')|\bar{c}\gamma_\nu b|\Lambda_b(p,s)\rangle &= \bar{u}(p',s')\left[f_1\gamma_\mu + f_2 v_\mu + f_3 v'_\mu\right]u(p,s)\,,\\
\langle\Lambda_c(p',s')|\bar{c}\gamma_\nu\gamma_5 b|\Lambda_b(p,s)\rangle &= \bar{u}(p',s')\left[g_1\gamma_\mu + g_2 v_\mu + g_3 v'_\mu\right]\gamma_5 u(p,s)\,,
\end{aligned} \tag{2.1}$$

where here $u$ and $v$ are Dirac spinors, while, $p$ and $s$ refer to 4-momentum and spin, respectively.

In the case of New Physics, several other potential interactions can be considered: Scalar, Pseudoscalar and Tensor. This in turn introduces Scalar ($h_S$), Pseudoscalar ($h_P$) and Tensor form factors ($h_1$, $h_2$, $h_3$ and $h_4$). The potential New Physics interactions can be parametrised in terms of their respective form factors in the following way:

$$\begin{aligned}
\langle\Lambda_c(p',s')|\bar{c}\,b|\Lambda_b(p,s)\rangle &= h_S\,\bar{u}(p',s')\,u(p,s)\,,\\
\langle\Lambda_c(p',s')|\bar{c}\gamma_5 b|\Lambda_b(p,s)\rangle &= h_P\,\bar{u}(p',s')\,\gamma_5\,u(p,s)\,,\\
\langle\Lambda_c(p',s')|\bar{c}\,\sigma_{\mu\nu}\,b|\Lambda_b(p,s)\rangle &= \bar{u}(p',s')\left[h_1\,\sigma_{\mu\nu} + i\,h_2(v_\mu\gamma_\nu - v_\nu\gamma_\mu) + i\,h_3(v'_\mu\gamma_\nu - v'_\nu\gamma_\mu)\right.\\
&\quad\left. + i\,h_4(v_\mu v'_\nu - v_\nu v'_\mu)\right]u(p,s)\,.
\end{aligned} \tag{2.2}$$

## 3. $\Lambda_b \to \Lambda_c\ell\nu$ using HQET

In the heavy quark limit a quark acts as a fixed colour source with fixed velocity [10]. This means that the wavefunction, which governs a hadron ($Qq$ or $Qqq'$) with a heavy quark, $Q$, is

| Decay | $N_{\rm IW}$ at $\mathcal{O}(1)$ | $N_{\rm SIW}$ at $\mathcal{O}(\Lambda_{\rm QCD}/m_{b,c})$ | $N_{\rm SIW}$ at $\mathcal{O}(\Lambda^2_{\rm QCD}/m_c^2)$ |
|---|---|---|---|
| $\Lambda_b \to \Lambda_c \ell^- \bar{\nu}_\ell$ | 1 | 0 | 2 |
| $B \to D^* l \nu$ | 1 | 3 | 6 |

**Table 1:** A comparison of the number of Isgur-Wise functions between semileptonic $\Lambda_b \to \Lambda_c$ transitions and $B \to D^{(*)}$ transitions within the HQET expansion at different orders.

insensitive to the spin and flavour of $Q$. Consequently, in the transition, $b \to c$ only the velocity change $v \to v'$ is felt and all form factors at leading order in the HQET expansion reduce to one universal function of $w = v \cdot v'$ known as the leading order Isgur-Wise (IW) function, $\zeta(w)$. More specifically at leading order the SM and NP form factors are given by,

$$\begin{aligned} &f_1(w) = g_1(w) = h_S(w) = h_P(w) = h_1(w) = \zeta(w)\,, \\ &f_2(w) = f_3(w) = g_2(w) = g_3(w) = h_2(w) = h_3(w) = h_4(w) = 0\,. \end{aligned} \tag{3.1}$$

Expanding to higher orders in $\alpha_s$, $\Lambda_{\rm QCD}/m_{b,c}$ and $\Lambda^2_{\rm QCD}/m_c^2$, an amazing simplification arises in the case of the baryonic $\Lambda_b \to \Lambda_c \ell^- \bar{\nu}_\ell$ decay with respect to its mesonic semileptonic $B \to D^*$ and $B \to D$ transitions. At order $\mathcal{O}(\Lambda_{\rm QCD}/m_{b,c})$ no new sub-leading Isgur-Wise functions enter compared to 3 for the mesonic transitions. Meanwhile, at order $\mathcal{O}(\Lambda^2_{\rm QCD}/m_c^2)$ just 2 sub-sub-leading IW functions are present compared to 6 for the mesonic transitions. Table 1 summarises the comparisons of the number of IW functions at different orders between baryonic and mesonic transitions. The decay $\Lambda_b \to \Lambda_c \ell^- \bar{\nu}_\ell$ is simpler as the light quarks ($ud$) are forced to be in a spin, $J = 0$, state since $J_{\Lambda_{b,c}} = 1/2$ and $J_{b,c} = 1/2$.

The expansion of $f_1$, at orders $\alpha_s$, $\Lambda_{\rm QCD}/m_{b,c}$ and $\Lambda^2_{\rm QCD}/m_c^2$, is given by,

$$f_1 = \zeta(w) \left\{ 1 + \hat{\alpha}_s C_{V_1} + \varepsilon_c + \varepsilon_b + \hat{\alpha}_s \left[ C_{V_1} + 2(w-1) C'_{V_1} \right] (\varepsilon_c + \varepsilon_b) + \frac{\hat{b}_1 - \hat{b}_2}{4 m_c^2} \right\} + \ldots\,, \tag{3.2}$$

where $\hat{\alpha}_s = \alpha_s/\pi$ and $\varepsilon_{c,b} = \bar{\Lambda}_\Lambda/(2 m_{c,b})$, in which $\bar{\Lambda}_\Lambda$ represents the energy of light degrees of freedom in the HQET expansion of $m_{\Lambda_Q} = m_Q + \bar{\Lambda}_\Lambda + \cdots$. At order $\mathcal{O}(\Lambda^2_{\rm QCD}/m_c^2)$, the shape dependence of the two additional sub-sub-leading IW functions is parametrised by the product of $I(w)$ and two additional functions, $\hat{b}_1(w)$ and $\hat{b}_2(w)$.

Further details of the expansions for the other functions can be found in Reference [9]. A similar expansion was performed for SM form factors previously in Reference [11].

## 4. HQET fit for the $\Lambda_b \to \Lambda_c \ell^- \bar{\nu}_\ell$ form factors

In order to more precisely determine the form factors of $\Lambda_b \to \Lambda_c \ell^- \bar{\nu}_\ell$ decays a $\chi^2$ fit combining inputs from both LQCD [5] and LHCb's differential shape measurement [7] was performed. The $\chi^2$ was computed according to,

$$\chi^2 = (\vec{\Gamma}_{\rm LHCb} - \vec{\Gamma}_{\rm HQET}(\vec{p}))^T \Sigma^{-1}_{\rm LHCb} (\vec{\Gamma}_{\rm LHCb} - \vec{\Gamma}_{\rm HQET}(\vec{p})) + \chi^2_{\rm LQCD}(\vec{p}) \tag{4.1}$$

where elements of the vector,

$$\hat{\Gamma}^i_{\mathrm{HQET}} = \frac{\int_{q^{2i}_{low}}^{q^{2i}_{up}} d\Gamma/dq^2}{\int_{q^2_{\min}}^{q^2_{\max}} d\Gamma/dq^2} , \tag{4.2}$$

are the normalised differential rate of $\Lambda_b \to \Lambda_c \mu^- \overline{\nu}_\mu$ integrated over given intervals in $q^2$ as determined from HQET, which are in turn functions of the HQET fit parameters $\vec{p}$. The term $\hat{\Gamma}^i_{\mathrm{LHCb}}$ and $\Sigma_{\mathrm{LHCb}}$ are the corresponding measured LHCb values and their associated covariance matrix. LHCb measured the normalised differential rate in several $q^2$ bins, which are normalized to unity reducing the effective degrees from 7 to 6. The term $\chi^2_{\mathrm{LQCD}}(\vec{p})$, which is given by

$$\chi^2_{\mathrm{LQCD}}(\vec{p}) = (\vec{f}_{\mathrm{LQCD}} - \vec{f}_{\mathrm{HQET}}(\vec{p}))^T \Sigma^{-1}_{\mathrm{LQCD}} (\vec{f}_{\mathrm{LQCD}} - \vec{f}_{\mathrm{HQET}}(\vec{p})) , \tag{4.3}$$

constrains the HQET computed form factors, $\vec{f}_{\mathrm{HQET}}(\vec{p})$, at chosen points in $q^2$ to those predicted from LQCD, $\vec{f}_{\mathrm{LQCD}}$. The LQCD form factor predictions were parametrised with either 11 or 17 parameters. Here the 6 form factors were evaluated using the 17 parameter parametrisation at three points in $q^2$ (1 GeV$^2$, $q^2_{\max}/2$ and $q^2_{\max}$), yielding 18 form factor values. The covariance matrix associated with the LQCD form factor values, $\Sigma^{-1}_{\mathrm{LQCD}}$, which is governed by the $17 \times 17$ covariance matrix of the LQCD form factor parameters, was evaluated using a Monte Carlo approach. Additionally, the difference between form factor values using the 17 and 11 parameter parametrisations is added as an uncorrelated uncertainty in the covariance matrix.

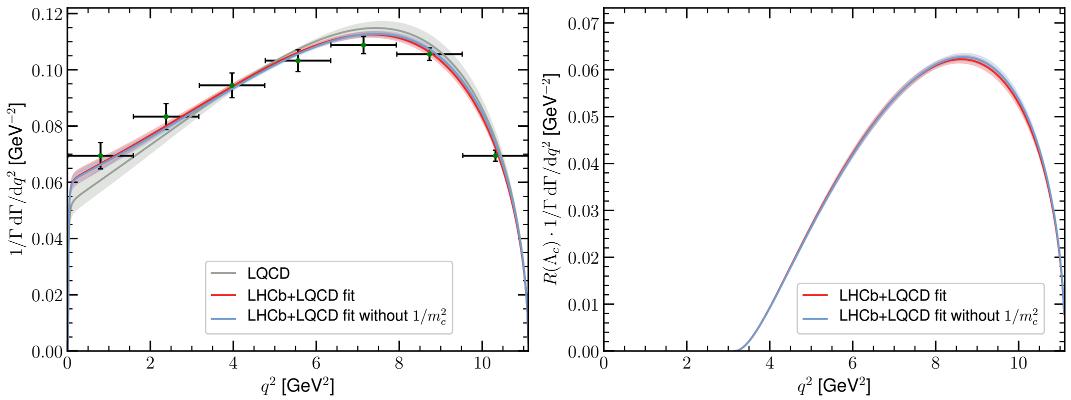


**Figure 1:** Normalised differential rate for $\Lambda_b \to \Lambda_c \mu^- \overline{\nu}_\mu$ (left) and $\Lambda_b \to \Lambda_c \tau^- \overline{\nu}_\tau$ (right) decays as predicted from the order $\mathcal{O}(\Lambda^2_{\mathrm{QCD}}/m_c^2)$ HQET fit. The predictions from LQCD and LHCb measured values are shown for $\Lambda_b \to \Lambda_c \mu^- \overline{\nu}_\mu$ decays as a dark grey line and points with error bars, respectively. Meanwhile, the red and blue curves show the predictions normalised from the higher and lower order HQET fits. The coloured bands display the uncertainties of the assoicated predictions.

In the fits the HQET expressions for the form factors are determined by parametrising the Isgur-Wise function according to a quadratic function of $w-1$,

$$\zeta(w) = 1 + (w-1)\,\zeta' + \frac{1}{2}(w-1)^2\,\zeta'' , \tag{4.4}$$

with two parameters $\zeta'$ and $\zeta''$. Meanwhile, the sub-sub-leading functions $\hat{b}_1$ and $\hat{b}_2$ are taken as being constants to be determined given the current level of sensitivity. Finally, $m_b^{1S}$ and $\delta m_{bc}$

| | including $\mathcal{O}(\Lambda^2_{\text{QCD}}/m_c^2)$ | neglecting $\mathcal{O}(\Lambda^2_{\text{QCD}}/m_c^2)$ |
|---|---|---|
| $\zeta'$ | $-2.04 \pm 0.08$ | $-2.06 \pm 0.08$ |
| $\zeta''$ | $3.16 \pm 0.38$ | $3.28 \pm 0.36$ |
| $\hat{b}_1/\text{GeV}^2$ | $-0.46 \pm 0.15$ | $0^*$ |
| $\hat{b}_2/\text{GeV}^2$ | $-0.39 \pm 0.39$ | $0^*$ |
| $m_b^{1S}/\text{GeV}$ | $4.72 \pm 0.05$ | $4.69 \pm 0.04$ |
| $\delta m_{bc}/\text{GeV}$ | $3.40 \pm 0.02$ | $3.40 \pm 0.02$ |
| $\chi^2/\text{ndf}$ | $7.20/20$ | $18.8/22$ |
| $R(\Lambda_c)$ | $0.3237 \pm 0.0036$ | $0.3252 \pm 0.0035$ |

**Table 2:** Summary of fit results when including or neglecting $\mathcal{O}(\Lambda^2_{\text{QCD}}/m_c^2)$ corrections.

are included in the fit but constrained to their measured values assuming Gaussian uncertainties. Thereby, the final parameter vector, $\vec{p}$ is given by $\{\zeta', \zeta'', \hat{b}_1, \hat{b}_2, m_b^{1S}, \delta m_{bc}\}$ for the case in which order $\mathcal{O}(\Lambda^2_{\text{QCD}}/m_c^2)$ terms are considered.

The results from fits including and neglecting $\mathcal{O}(\Lambda^2_{\text{QCD}}/m_c^2)$ terms are shown in Table 2, while, Figure 1 shows the resulting predictions for the normalised differential rate of $\Lambda_b \to \Lambda_c \mu^- \overline{\nu}_\mu$ and $\Lambda_b \to \Lambda_c \tau^- \bar{\nu}_\tau$ decays. The ratio $R(\Lambda_c) = 0.3237 \pm 0.0036$ is determined, which is the most precise determination to date. Figure 2 compares predictions from the HQET fits for each SM form factor with those from LQCD. For the form factor $g_1$ order $\mathcal{O}(\Lambda^2_{\text{QCD}}/m_c^2)$ terms are necessary to match the LQCD predictions.

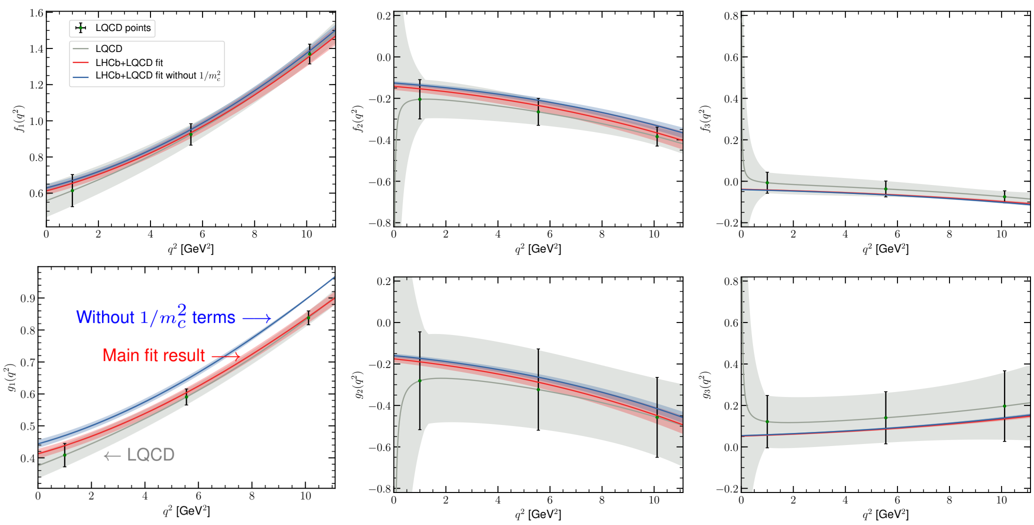


**Figure 2:** Comparison of the SM form factors determined from the HQET fit to the corresponding LQCD predictions. The points with error bars indicate the form factor values used in the fit and their corresponding uncertainties.



PoS(EPS-HEP2019)265

## 5. Sensitivity to new physics

Using the fitted parameters from the SM fit one is able to determine the NP form factors as these are expressed in terms of the same IW functions. Figure 3 shows a comparison of the NP form factors as predicted by the HQET fits and by LQCD. The poor agreement between LQCD and the HQET fit for the tensor form factor $h_1$ is yet to be understood.

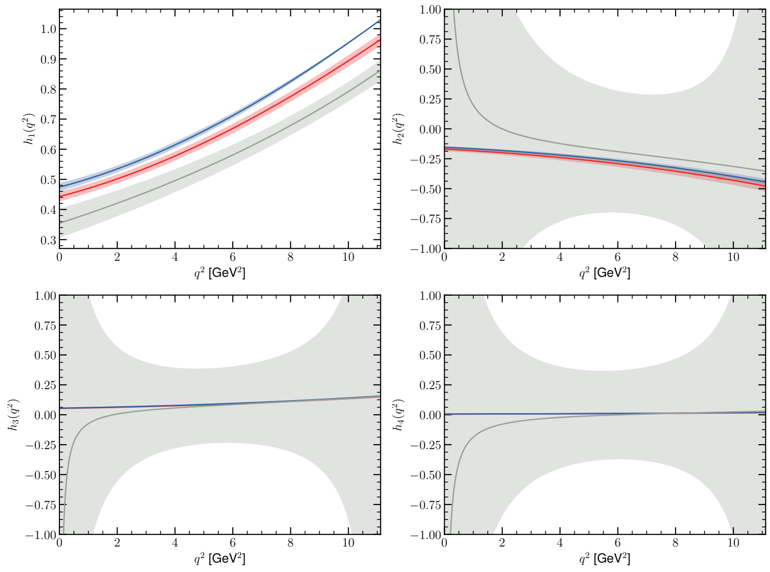


**Figure 3:** Comparison of the NP factors determined from the HQET fit to the corresponding LQCD predictions.

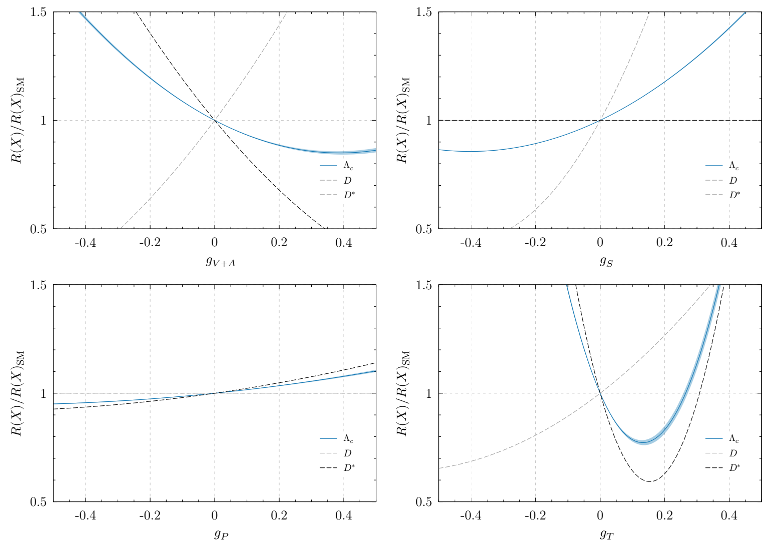


**Figure 4:** Dependence of of $R(X)_{\rm NP}/R(X)_{\rm SM}$ with $X = \Lambda_c, D^*, D$ on a variety of NP coupling strengths.

The predictions for the NP form factors can be used to determine the sensitivity of $R(\Lambda_c)$ to various possible New Physics interactions. Figure 4 shows how the ratio of $R(X)_{\mathrm{NP}}/R(X)_{\mathrm{SM}}$ for $X = \Lambda_c, D^*, D$ varies with the coupling strength of potential vector, scalar, pseudoscalar and tensor interactions.

## 6. Conclusion and outlook

In these proceedings earlier work from References [8, 9] was summarised, in which a fit combining LQCD form factor predictions and a differential rate measurement from LHCb was performed in order to more precisely determine the form factors of $\Lambda_b \to \Lambda_c \ell^- \bar{\nu}_\ell$ decays. The fit utilised the framework of HQET, within which the SM form factors were computed up to order $\mathcal{O}(\Lambda^2_{\mathrm{QCD}}/m_c^2)$. This allowed for the first quantification of the magnitude of order $\mathcal{O}(\Lambda^2_{\mathrm{QCD}}/m_c^2)$ terms in the HQET expansion, with $\hat{b_1} = -0.46\ \mathrm{GeV}^2$. Furthermore, utilsing the best fit parameters a new prediction of $R(\Lambda_c) = 0.324 \pm 0.004$ was computed, which is the most precise theoretical prediction for $R(\Lambda_c)$ to date. In addition to the SM form factors, the NP physics form factors were computed for the first time to order $\mathcal{O}(\Lambda^2_{\mathrm{QCD}}/m_c^2)$ in Reference [9], which allowed the sensitivity of $R(\Lambda_c)$ to a range of NP scenarios to be investigated.

## References


[1] G. Ciezarek *et al* *Nature* **546** (2017) 227-233

[2] F. Archilli *et al* *Nature* **546** (2017) 221-226

[3] HFLAV, (2018) [arXiv:1909.12524v1]

[4] P. Boer *et al*, *JHEP* **06** (2018) 155

[5] S. Meinel, D. Detmold, C. Lehner, *Phys. Rev.* **3** (2015) 034503

[6] S. Meinel, A. Datta, S. Kamali, A. Rashed, *JHEP* **08** (2017) 131

[7] LHCb Collaboration, *Phys. Rev.* **D96** (2017) 112005

[8] F. Bernlochner, Z. Ligeti, D. Robinson, W. Sutcliffe, *Phys. Rev.* **D96** (2018) 112005

[9] F. Bernlochner, Z. Ligeti, D. Robinson, W. Sutcliffe, *Phys. Rev. D* **99** (2019) 055008

[10] N. Isgur, M. Wise, *Phys. Lett.* **B232** (1989) 113-117

[11] A. Falk, M. Neubert, *Phys. Rev.* **D47** (1993) 2982-2990